Chemical Design and Thin Film Preparation of *p*-Type Conductive Transparent Oxides

HIROSHI YANAGI, HIROSHI KAWAZOE, ATSUSHI KUDO, MASAHIRO YASUKAWA
& HIDEO HOSONO

Materials and Structures Laboratory, Tokyo Institute of Technology 4259 Nagatuta, Midori-ku, Yokohama 226-8503, Japan

Abstract. Chemical design to find a new transparent conductive oxide having *p*-type conductivity has been proposed. Following the chemical design, we have selected $CuGaO_2$ and $CuAlO_2$ as candidate materials. $CuGaO_2$ thin films were prepared on silica glass substrates by RF sputtering method. The optical band gap of the film was estimated to be ~ 3.4 eV. Positive sign of Seebeck coefficient demonstrated the *p*-type conductivity of the film. The dc conductivity of the film was 5.6×10^{-3} S·cm^{-1} and the activation energy was 0.22 eV at room temperature. Because of rough texture of the film, the observed conductivity was not an intrinsic property of the material. Further, $CuAlO_2$ thin films were prepared by laser ablation. The film deposited in O_2 atmosphere of 1.3 Pa at $690°C$ showed higher optical transmission in visible and near-infrared regions than previously reported. Contribution of Cu 3d components to upper edge of valence band in $CuGaO_2$ and $CuAlO_2$ were confirmed by photoemission spectroscopic measurements.

Keywords: p-type conductor, transparent oxide, delafossite

1. Introduction

A series of doped oxides of *p*-block elements such as aluminum doped zinc oxide (AZO), tin doped indium oxide (ITO) and antimony doped tin oxide (ATO) have a unique characteristic that dc electrical conductivity can be controlled from that of an insulator to that of a metal, while thin films of the materials are transparent in visible range. The materials, therefore, have been one of essential components in flat panel displays and solar cells as a metallic lead.

Notwithstanding their extraordinarily wide controllable conductivity range including that of semiconductor, the applications are limited to the transparent electrodes. It seems to us that origin of the limited application is due to lacking of *p*-type conducting transparent oxide materials. *p-n* junction can not be fabricated totally from the transparent oxides. It is needless to say that the junction is a key structure in most of semiconductor devices.

We have proposed chemical design of the *p*-type conducting and transparent oxides and found that the properties are possessed by some oxides. In the present paper, details of the chemical design, thin film preparation of candidate oxides, and the results of structure analysis and physical property measurements are reported.

2. Chemical Design

In this section, discussed will be necessary requirements in the electronic energy band structure, chemical composition and crystal structure which must be possessed by the candidate oxides.

As the starting point of the discussion we must understand semi-quantitatively the origin which suppresses formation of *p*-type conductive wide band gap oxides. Generally, because of large electronegativity of oxygen, the valence band edge

of oxides is strongly localized on oxygen ion. In chemical terminology, it is called a lone pair electron. Then the positive holes introduced at the edge are localized on oxygen ion(s) and constitute a deep trap, such as ZnO:Na [1]. The positive holes can not migrate within the crystal even under an applied electric field. Therefore, modulation or modification of the energy band structure to reduce the localization of the valence band edge has a primary importance in the chemical design of *p*-type conductive wide gap ionic solid.

How we can solve the problem. A possible method of the modulation is shown in Fig. 1. Here the cation species are assumed to have a closed shell electronic configuration whose energy is comparable to 2 p electrons on oxygen ions. The closed shell is required to avoid optical absorption in visible range. In this combination considerable covalency can be expected for both the bonding and anti-bonding levels. The valence band edge shifts from the 2 p levels of oxygen ions to the anti-bonding levels because both the cation and anion have closed shell electronic configuration. It should be noted that the localization nature of the valence band edge is greatly reduced by the modification.

Next problem is how we can find out the cationic species that satisfy with the scheme shown in Fig. 1. We found a possible solution accidentally in the course of study on *n*-type conducting wide gap oxides. Figure 2 displays photoemission spectrum of $CdIn_2O_4$ spinel obtained by using synchrotron radiation as an excitation $(h\nu = 60\,\text{eV})$. This material has been known to be an *n*-type conducting degenerate semiconductor [2], and the Fermi level, which is set to 0 in the energy scale, is locating in the conduction band edge. As stated previously, the valence band edge located around 4.5 eV is mostly due to oxygen 2 p electrons in the oxide. There are two additional
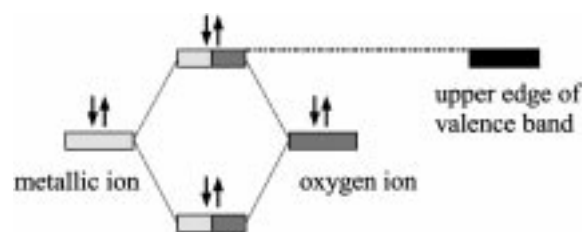

Fig. 1. Schematic diagram of modulation of band structure. Cations are assumed to have a closed shell the energy of which is equivalent to that of O $2\,p^6$.
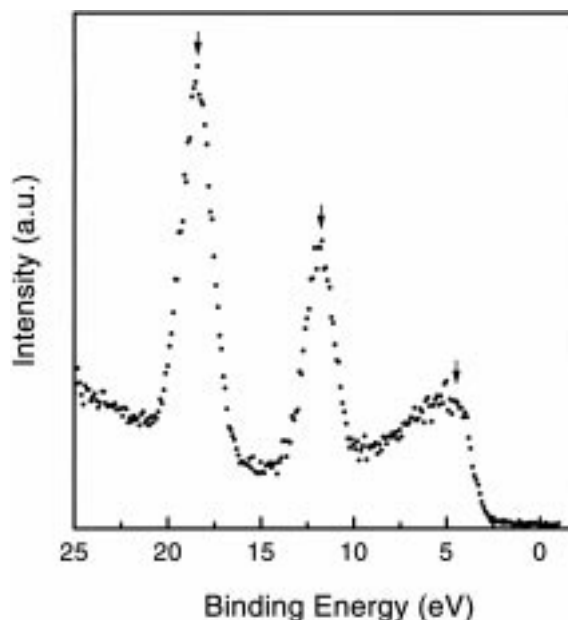

Fig. 2. Photoemission spectrum of the valence region of degenerated $CdIn_2O_4$ excited at $h\nu = 60\,\text{eV}$.

and rather distinct peaks at around 11.7 eV and 18.2 eV. These are assigned to semi inner shell $4\,d^{10}$ electrons of Cd^{2+} and In^{3+} ions. The energy difference between the two distinct peaks is estimated to be $\sim 6.5\,\text{eV}$, and that between oxygen 2 p (valence band edge) and $4\,d^{10}$ of Cd^{2+} is $\sim 7\,\text{eV}$. If we notice that Cd and In are neighboring elements in the periodic table and the energy of a particular atomic orbital goes into deep with increasing atomic number, the solution to find out the candidate species is easily found.

In Fig. 3 changes in the energy of $4\,d^{10}$ electrons on some elements including Cd and In with increasing atomic number is displayed. These are calculated values for independent atomic state [3]. The difference in the energies of $4\,d^{10}$ electrons on Cd and In is estimated to be $\sim 5\,\text{eV}$, which is very close to that observed for the ionized species in $CdIn_2O_4$. It is reasonably assumed that the energy difference itself is retained even in the ionized states. We are looking for the cation with the closed shell whose energy is $\sim 7\,\text{eV}$ higher than that of $4\,d^{10}$ on Cd^{2+}. From the figure, the possible solution is found to be monovalent silver, Ag^+, its $4\,d^{10}$ electrons being expected to be very close to that of O 2 p. This argument can be applied also to the corresponding 3d elements as seen in the figure, and Cu^+ is found to be another candidate.
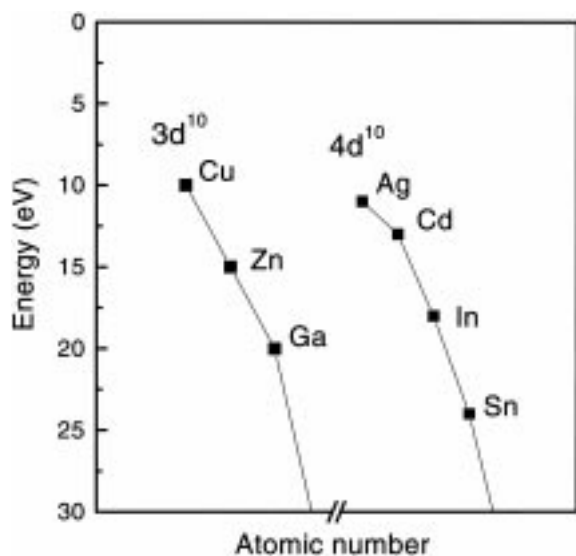
Final requirement on the crystal structure concerns capability of substitutional doping and possibility of n-type conductivity, which facilitate fabrication of *p-n* junction and semiconductor devices.

3. Selection of Materials

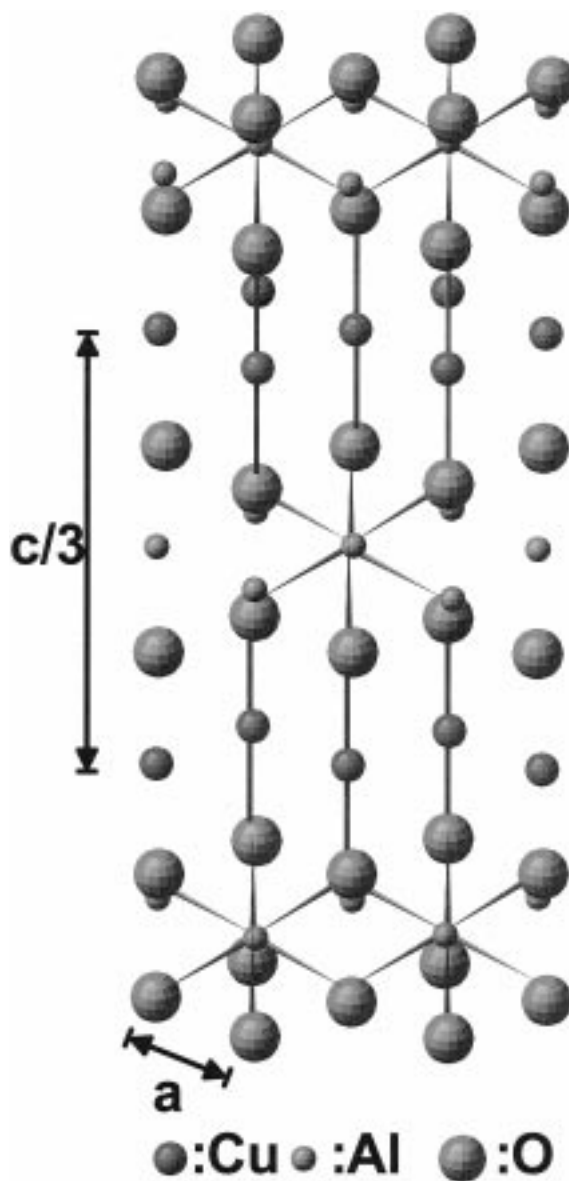Taking the above stated requirements into consideration, we have selected as candidate materials gallate

Fig. 3. Changes in the energies of $3d^{10}$ and $4d^{10}$ electrons on some elements with increasing atomic number.

The second part of the chemical design is the consideration of the crystal structure advantageous for the *p*-type conductivity. At this stage we could understand Cu_2O [4] and Ag_2O have been known *p*-type conductive oxides, but they have strong color, the band gap being reported to be $\sim 2\,eV$ [5]. Some favorable structural characteristics are extracted from Cu_2O. Oxygen ions in the structure are in tetrahedral coordination. This seems to be advantageous in reducing the localization of the valence band edge. Valence state of oxygen ions is approximately shown as sp^3 and the eight electrons constitute σ bondings with the four neighboring cations. In chemical terminology, there is no non-bonding electron.

Linear coordination of two oxygen ions to Cu^+ ion may be an indication of the fact that $4\,d^{10}$ electrons on Cu^+ have comparable energy with O 2p electrons: $4\,d^{10}$ electrons surrounding Cu^+ have strong repulsion energy with O 2p, and oxygen ions cannot approach to the Cu^+ ions. Therefore, the linear conformation of Cu^+ is also favorable.

Cu^+ ions in the structure have three-dimensional interactions with the nearest neighboring Cu^+ ions. It might be possible that the repulsive interactions between the Cu^+ ions expand band width and reduce band gap energy. Thus lower dimensional structure, which reduces the repulsive interactions between the Cu^+ ions, might be favorable for enlarging band gap for transmitting visible light.

Fig. 4. Crystal structure of delafossite consisting of stacked layers of -O-Ga(Al)-O-Cu-O- in this order along the *c*-axis.

and aluminate of Cu^+, $CuGaO_2$ and $CuAlO_2$ [6,7] with delafossite structure, whose crystal structure is shown in Fig. 4. Local symmetries around Cu^+ and O^{2-} ions in this phase are the same as those in Cu_2O, except the nearest neighboring cations of the oxygen ion are one Cu^+ and three Ga^{3+} or Al^{3+} in the delafossites. The structure can be viewed as the layer structure in the sequence of Cu-O-Ga(Al)-O-Cu along the c-axis, and the three-dimensional crosslinking of Cu^+ network seen in Cu_2O is reduced to two-dimensional. This might give rise to a larger band gap of the delafossite compared to that of Cu_2O.

The other candidate material for p-type conductive oxide with wide band gap is $SrCu_2O_2$. This crystal has O-Cu-O dumbbell structure as that of Cu_2O. The dumbbell structure units are connected to form zigzag shape one-dimensional chain along with [1 0 0] and [0 1 0] directions at the angle of $96.25°$. The dimension of electronic interaction of Cu^+ with nearest neighboring Cu^+ is reduced within a single chain compared with three-dimensional structure in Cu_2O. This might give rise to a larger band gap of $SrCu_2O_2$ than that of Cu_2O. The details of p-type conductivity of $SrCu_2O_2$ thin films were reported by Kudo et al. [8].

4. Experimental

4.1. Sample Preparation

Polycrystalline thin films of $CuGaO_2$ were prepared by RF sputtering method. Sintered disks for target materials in the sputtering and photoemission measurements of $CuGaO_2$ were prepared by using solid state reactions of Cu_2O and Ga_2O_3 [9]. Stoichiometric amounts of the raw materials were mixed thoroughly with using methanol vehicle and pre-heated under nitrogen atmosphere at $1100°C$ for 24 h. The material was pelletized, cold-isostatic pressed and sintered at $1100°C$ for 24 h under nitrogen atmosphere. Apparent density of the disks was about 75% of the theoretical one.

Sputtering conditions employed were total pressure; 0.1 Torr, sputtering gas ratio of Ar/O_2; 40/10, substrate material; synthetic silica glass, substrate temperature; room temperature, and RF power; 180 W. The deposited film was obtained in amorphous state, and was subjected to post-annealing for crystallization at $850°C$ for 12 h under nitrogen atmosphere.

Polycrystalline thin films of the $CuAlO_2$ were prepared by laser ablation. Sintered disks were used as a target material. The disks were prepared by using solid-state reactions of Cu_2O and Al_2O_3 [10]. Preparation conditions used in the laser ablation were as follows. Excitation: pulses from a KrF excimer laser, 248 nm, 20 Hz, and $5\,J\cdot cm^{-2}$ per pulse (Lambda Physik Compex 102); substrate: single-crystalline sapphire with c surface orientation (0 0 0 1); temperature: $690°C$; base pressure: 10^{-6} Pa; atmosphere: oxygen with a pressure of 1.3 Pa. The films were annealed at deposition temperature for 3 h after the deposition, and cooled to room temperature keeping the deposition oxygen pressure.

4.2. Structure and Property Determination

The crystalline phases in the films and the sintered disks were identified by X-ray diffraction (Cu Kα: Rigaku Rint-2500), and film thickness was estimated by using a stylus (Sloan DEKTAK^{3}ST). The electrical conductivity of thin films was measured by two-probe method at the temperatures ranging from 60 K to 300 K. Optical transmission spectra of the thin films were measured in the wavelength range from 185 to 3200 nm with a dual beam spectrophotometer (Hitachi U-4000).

Photoemission measurements on $CuGaO_2$ were done at room temperature on the ceramic samples at BL2B1 and BL8B2 beamlines in UVSOR installed in Institute for Molecular Science. The excitation energies were varied from 65 eV to 90 eV. Surface of the ceramic samples was ground by a diamond file in a preparation chamber under 8×10^{-7} Pa just before the measurements and the samples were transferred to a measurement chamber with a vacuum of 5×10^{-8} Pa. Similarly prepared Cu_2O sintered disk (apparent density of 90%) was subjected to similar photoemission measurements for comparison.

Photoemission and inverse photoemission measurements on $CuAlO_2$ were carried out at room temperature on the thin film samples using an instrument built up in our laboratory. This instrument is equipped with facilities for X-ray and ultraviolet photoemission spectroscopy (XPS and UPS) and bremsstrahlung isochromat spectroscopy (BIS), which belongs to inverse photoemission spectroscopy (IPES) techniques. In the photoemission measurement, the excitations used were He II resonance radiation (40.8 eV) and Mg Kα X-ray (1254 eV). The

facility for BIS measurement detects 9.4 eV photons by electron multiplier (Hamamatsu Photonics: R595) through a SrF_2 single crystal window. Photoemission and BIS spectra were measured under the vacuum level of 1×10^{-7} Pa and 5×10^{-8} Pa, respectively.

5. Results

5.1. Composition and Structure Analysis

Chemical analyses of $CuGaO_2$ delafossite samples by inductively coupled plasma method gave Ga/Cu atomic ratio in the sintered body and thin film to be 1.04 and 0.97, respectively. These were in satisfactory agreement with the stoichiometric ratio from the interest of the phases obtained.

Figure 5 shows X-ray powder diffraction patterns of the $CuGaO_2$ and $CuAlO_2$ in the forms of sintered ceramics and post-annealed thin films. All diffraction peaks seen in the patterns of the sintered ceramics and thin films could be indexed by assuming delafossite structure. As-deposited films of the $CuGaO_2$ were in amorphous state as far as X-ray diffraction concerned, but crystallized during the post-annealing. All trials were unsuccessful to obtain a polycrystalline thin film on glass substrate in as-deposited state by changing substrate temperature, sputtering gas, or RF power. X-ray diffraction indicated low crystallinity or small grain size in the thin films. These structural characteristics are disadvantageous in electrical conduction.

5.2. Photoemission Measurements on $CuGaO_2$

Photoemission spectra were measured by using synchrotron radiation as an excitation light in order to estimate semi-quantitatively contribution of Cu 3d components to the upper edge of valence band in Cu_2O and $CuGaO_2$. The resonance enhancement of the satellite peak usually appears around 15 eV and the photoemission intensity of the upper valence bands decrease simultaneously [11].

The wide binding energy spectrum of Cu_2O obtained by 76 eV excitation was exactly the same with that reported by Thuler et al. [11]. The satellite band was detected at 15.2 eV. The topmost occupied band at 1.1 eV started to rise from almost 0 binding energy, which was an experimental indication of the fact that the material is a p-type semiconductor. It is noted that the satellite peak was enhanced at 76–79 eV excitation energies, whereas intensity of the uppermost band at 1.1 eV was decreased at the same excitation energy region. The observation is almost the same with that reported by Thuler et al. [11]. The concerted excitation energy dependence of the satellite and uppermost peaks did show that contribution of Cu 3d is significant in the upper valence band.

The wide range photoemission spectrum of $CuGaO_2$ obtained by 130 eV excitation is displayed in Fig. 6. The valence band edge started around 0.5 eV, this suggesting the material to be a p-type conductor. Two sharp peaks seen at 20–25 eV range were assigned to Ga $3d_{5/2}$ (D) and $3d_{3/2}$ (E) emissions. In the valence region two peaks and a shoulder were observed at 3.5 eV (A), 6.5 eV (B), and 9.5 eV (C), respectively. The semi-quantitative estimation of the contribution of Cu 3d to the topmost bands is the central concern. A tail of the Ga $3d_{5/2}$ peak accidentally overlapped with the satellite peak, but estimation of the excitation energy dependence of the intensity of the satellite peak was still reliable. The dependence of the topmost band (A) and satellite peak is shown in Fig. 7. The almost similar dependence was observed with Cu_2O. Therefore, we might say that several tens% of contribution of Cu 3d component to the top of valence band was experimentally evidenced.
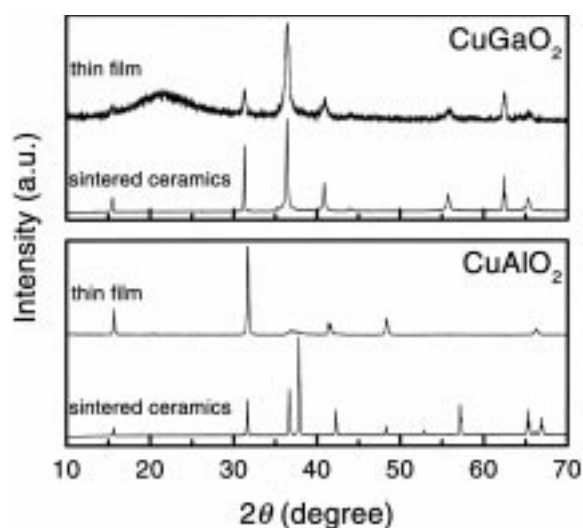
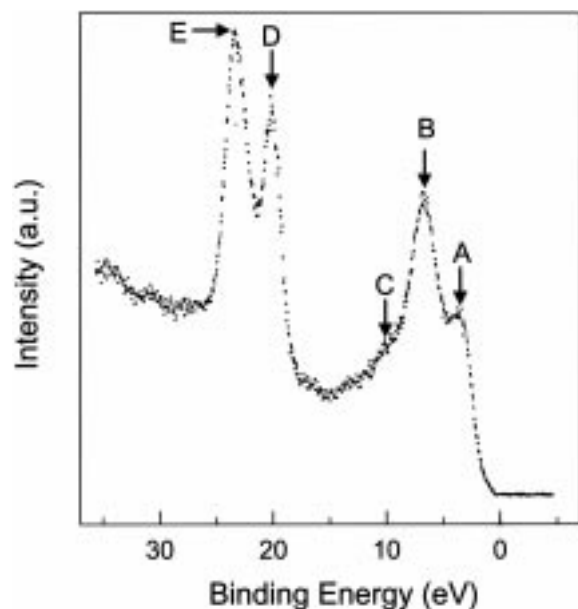*Fig. 5.* X-ray diffraction patterns of the delafossite, $CuGaO_2$ (upper panel) and $CuAlO_2$ (lower panel).

Fig. 6. Photoemission spectrum of the valence region of $CuGaO_2$ excited at $h\nu = 130\,\text{eV}$.

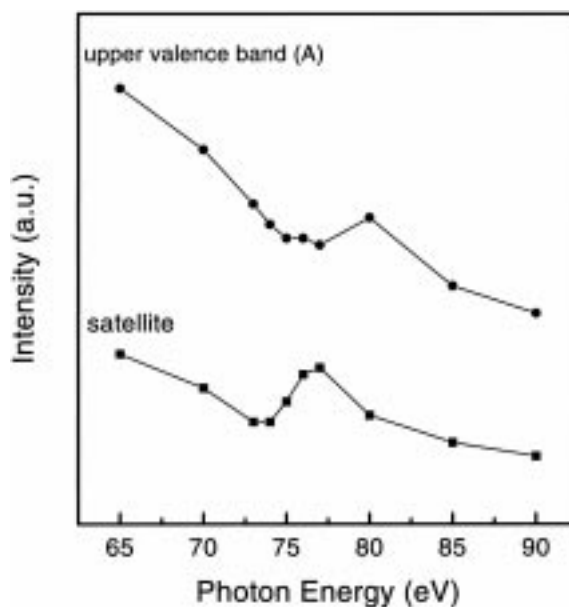## 5.3. *Photoemission and Inverse Photoemission Measurements on* $CuAlO_2$

XPS, UPS and BIS spectra were measured by using a home-built apparatus. Figure 8 shows PES and BIS spectra of $CuAlO_2$. It is noted that the intensities of each spectrum are determined independently. The Fermi energy determined experimentally was set to zero in the energy scale in the three spectra. A band gap was observed between the valence band edge in the PES spectra and the conduction band edge in the BIS spectrum. The band gap estimated was about 3.5 eV. The Fermi energy lies around the top of the valence band. This observation agrees with the fact that the sample is a *p*-type semiconductor [7].

In order to estimate contribution of Cu 3d components to the upper edge of valence band in $CuAlO_2$, photoemission spectra were measured by using two different excitation lights; 40.8 eV (He II resonance radiation) and 1254 eV (Mg Kα X-ray). The ratio of the emission cross section of Cu 3d/O 2 p at 40.8 eV excitation is about 1.5. On the other hand, the ratio at 1254 eV is about 30. The relative intensity of the occupied band observed at 4.0 eV in UPS spectrum increased greatly in XPS spectrum. This shows that contribution of Cu 3d is significant in the upper valence band.

Fig. 7. Excitation energy dependence of the intensity of the satellite peak and upper valence peaks in $CuGaO_2$.

5.4. *Optical and Electrical Properties*

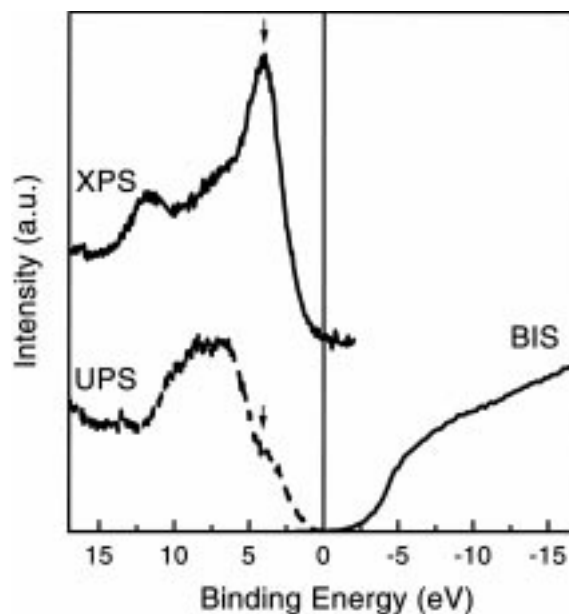The as-deposited film of $CuGaO_2$ was brown-black in color and no transparent wavelength range was found

Fig. 8. Photoemission and inverse photoemission spectra of the valence and conduction region of $CuAlO_2$.

in visible and NIR region. No distinct peak was detected in the X-ray diffraction pattern of the as-deposited film, and metallic colloid particles are excluded from the possible origins of the coloration. No ESR absorption due to Cu^{2+}, irrespective of its chemical state such as isolated ion, magnetically interacting (closely neighboring) Cu^{2+} ions, or Cu^+-Cu^{2+} mixed valence state, was detected. Chemical origin, therefore, of the black coloration in the as-deposited film is not clear at present.

Optical absorption spectra of the post-annealed $CuGaO_2$ thin film and $CuAlO_2$ thin film in visible and NIR region is displayed in Figs. 9 and 10, respectively. The $CuGaO_2$ film has a color of yellow. Accordingly the fundamental optical absorption starts from about 350 nm. The inset of Fig. 9 shows $(\alpha h\nu)^2$-$h\nu$ plot for estimating the direct allowed band gap, and it was found to be about ~ 3.4 eV. However diffuse reflectance spectrum showed small absorption band around 650 nm, and indirect band gap may be smaller than 3.4 eV [12].

The transmittance of the $CuAlO_2$ film is around 70% in visible region. The direct allowed band gap estimated by $(\alpha h\nu)^2$-$h\nu$ plot was found to be about ~ 3.5 eV. This value agrees with the band gap estimated from PES and IPES spectra.

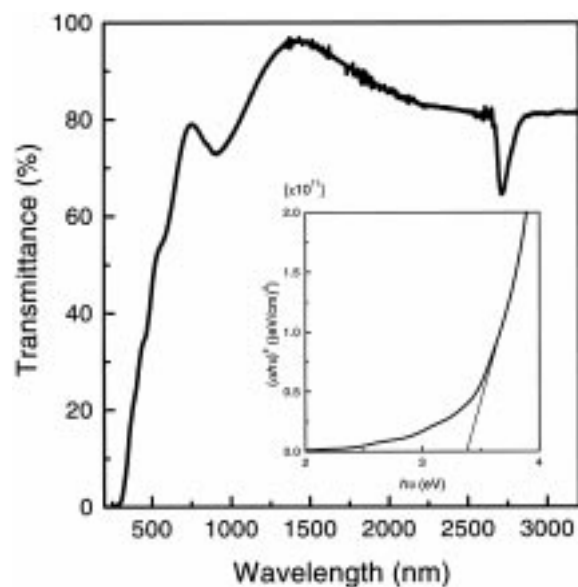Temperature dependence of electrical conductivity

Fig. 10. Optical transmission spectrum of $CuAlO_2$ thin film.

of $CuGaO_2$ and $CuAlO_2$ thin films is shown in Fig. 11. Semiconductive temperature dependence was noticed. For $CuGaO_2$ thin film roughly estimated activation energy was 0.22 eV. The conductivity at room temperature was about 5.6×10^{-3} S·cm^{-1}.

Fig. 9. Optical transmission spectrum of $CuGaO_2$ thin film. The inset shows the plot of $(\alpha h\nu)^2$ against $h\nu$ for estimation of direct allowed optical gap.
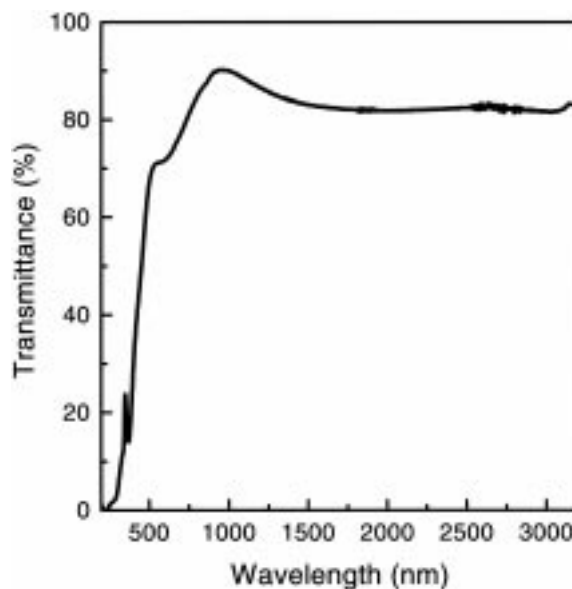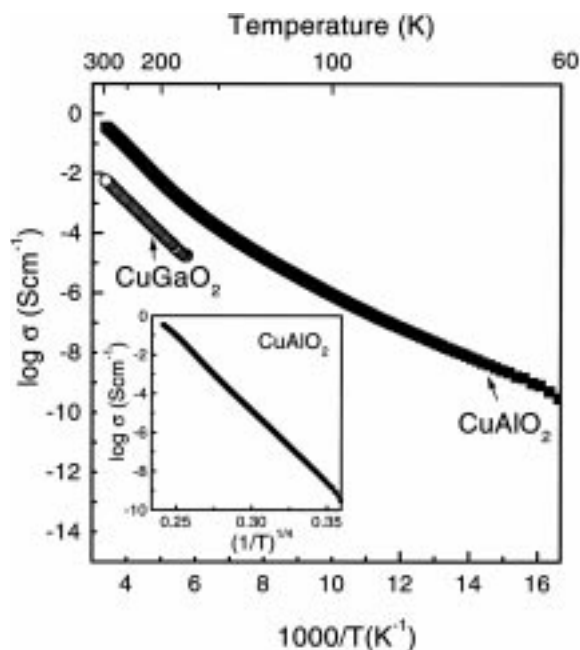

Fig. 11. Temperature dependence of dc electrical conductivity of $CuGaO_2$ and $CuAlO_2$ thin films. The inset shows $T^{1/4}$ plot of $CuAlO_2$.

Seebeck coefficient at room temperature was found to be $+230\,\mu V \cdot K^{-1}$. Its positive sign indicates that the CuGaO$_2$ thin film is a *p*-type conductor. Hall voltage could not be measured.

For CuAlO$_2$ thin film semiconductive temperature dependence was noticed in the range from 300 K to 220 K the roughly estimated activation energy was 0.22 eV. At lower temperatures, below 220 K, conductivity followed almost a $T^{-1/4}$ rule, as seen in the inset. This suggests that a variable-range hopping mechanism is dominant at lower temperatures. The conductivity at room temperature was about $3.4 \times 10^{-1}\,S \cdot cm^{-1}$. We have already reported CuAlO$_2$ thin film is *p*-type conductor [7].

6.   Discussion

In the present study it is aimed to establish an approach for finding a transparent and *p*-type conductive materials. We have successfully confirmed *p*-type conductivity of CuGaO$_2$ thin film by the measurements of Seebeck coefficient. The conductivity was $5.6 \times 10^{-3}\,S \cdot cm^{-1}$. Further, we ascertained CuAlO$_2$ and SrCu$_2$O$_2$ thin films to be *p*-type transparent conductive oxides in previous papers [7,8]. These materials were selected from the considerations on requirements on electronic structures and atomic arrangements. The central idea proposed for finding *p*-type conductive and wide gap material is mixing of O 2 p with the filled d^{10} band of Cu$^+$ or Ag$^+$, to suppresses nonbonding nature of the valence band edge energy.

Photoemission spectra of CuGaO$_2$ and CuAlO$_2$ thin films indicate experimentally that Cu 3d component exists in the top of valence bands, though the valence band edge of most of wide gap oxides are mainly constituted by oxygen 2 p electrons. That is to say, modulation or modification of the energy band structure to reduce the localization of the valence band edge could be realized on these materials.

Transmittance of CuAlO$_2$ thin film is improved from the previously reported [7]. For example, transmittance was increased from $\sim 70\%$ to $\sim 80\%$ in NIR and from 36% to 67% at 500 nm, the conductivity being without significant difference.

References

1. D. Zwingel and F. Gärtner, *Solid State Comm.*, **14**, 45 (1974).
2. T. Omata, N. Ueda, N. Hikuma, K. Ueda, H. Mizoguchi, T. Hashimoto, and H. Kawazoe, *Appl. Phys. Lett.*, **62**, 5 (1993).
3. D. DeVaut, *J. Chem. Educ.*, **21**, 575 (1944).
4. L. Kleinman and K. Mednick, *Phys. Rev. B.*, **21**, 1549 (1980).
5. M. Hayashi and K. Katsuki, *J. Phys. Soc. Jpn.*, **5**, 380 (1950).
6. R.D. Shannon, D.B. Rogers, and C.T. Prewitt, *Inorg. Chem.*, **10**, 713 (1971).
7. H. Kawazoe, M. Yasukawa, H. Hyodo, M. Kurita, H. Yanagi, and H. Hosono, *Nature*, **389**, 939 (1997).
8. A. Kudo, H. Yanagi, H. Hosono, and H. Kawazoe, *Appl. Phys. Lett.*, **73**, 220 (1998).
9. K.T. Jacob and C.B. Alcock, *Rev. int. Htes. Temp. et Refract.*, **13**, 37 (1976).
10. T. Ishiguro, A. Kitazawa, N. Mizutani, and M. Kato, *J. Solid State Chem.*, **40**, 170 (1981).
11. M.R. Thuler, R.L. Benbow, and Z. Hurych, *Phys. Rev. B.*, **26**, 669 (1982).
12. F.A. Benko and F.P. Koffyberg, *Phys. Stat. Sol.*, **94**, 231 (1986).